Catheter contact angle influences local impedance drop during radiofrequency catheter ablation: Insight from a porcine experimental study with 2 different LI-sensing catheters

Gen Matsuura[1], Hidehira Fukaya[1], Emiyu Ogawa[1], Sota Kawakami[1], Hitoshi Mori[2], Daiki Saito[1], Tetsuro Sato[1], Hironori Nakamura[1], Naruya Ishizue[1], Jun Oikawa[1], Jun Kishihara[1], Shinichi Niwano[1], and Junya Ako[1]

[1]Kitasato University School of Medicine
[2]Saitama Medical University International Medical Center

September 25, 2021

Abstract

Background: Local impedance (LI) can indirectly measure catheter contact and tissue temperature during radiofrequency catheter ablation (RFCA). However, data on the effects of catheter contact angle on LI parameters are scarce. This study aimed to evaluate the influence of catheter contact angle on LI changes and lesion size with 2 different LI-sensing catheters in a porcine experimental study. Methods: Lesions were created by the INTELLANAV MiFi OI (MiFi) and the INTELLANAV STABLEPOINT (STABLEPOINT). RFCA was performed with 30 watts and a duration of 30 seconds. The CF (0, 5, 10, 20, and 30 g) and catheter contact angle (30°, 45°, and 90°) were changed in each set (n=8 each). The LI rise, LI drop, and lesion size were evaluated. Results: The LI rise increased as CF increased. There was no angular dependence with the LI rise under all CFs in the MiFi. On the other hand, the LI rise at 90° was lower than at 30° under 5 and 10 g of CF in STABLEPOINT. The LI drop increased as CF increased. Regarding the difference in catheter contact angles, the LI drop at 90° was lower than that at 30° for both catheters. The maximum lesion widths and surface widths were smaller at 90° than at 30°, whereas there were no differences in lesion depths. Conclusion: The LI drop and lesion widths at 90° were significantly smaller than those at 30°, although the lesion depths were not different among the 3 angles for the MiFi and STABLEPOINT.

Introduction

Radiofrequency (RF) catheter ablation (CA) is an established treatment for several types of cardiac arrhythmias. [1]Creating sufficient lesion formation is crucial for successful ablation. In contrast, excessive RF delivery can lead to steam pops or perforations;[2] therefore, it is paramount to energize without excess or deficiency.

Recently, contact force (CF) sensing catheters have become the standard tools for RFCA,[3] [4] [5] and CF parameter-integrated indices, such as the force-time integral (FTI),[6] ablation index (AI),[7] [8] and lesion size index (LSI)[9], have been reported as effective surrogate parameters for sufficient lesion creation, especially in pulmonary vein isolation (PVI) for atrial fibrillation (AF). However, these indices are provided only from the ablation parameters and do not include the characteristics of the local myocardial tissue.

Historically, generator impedance change has been used as a surrogate marker of lesion creation by an RF application;[10] however, since the absolute value of the change is crude, it cannot be used as a definitive marker of lesion formation. Recently, a local impedance (LI) detectable ablation catheter (INTELLANAV MiFi OI, Boston Scientific, Maple Grove, MN, USA: MiFi) was put on the market. This catheter has 3 microelectrodes incorporated into the distal tip, and a more precise LI would be detected with these microelectrodes. Since the LI would be changed by tissue contact and temperature, this parameter allows us to speculate about the CF and tissue temperature during the RF application[11]. In addition, both LI- and CF-sensing ablation catheters (INTELLANAV STABLEPOINT Boston Scientific, Maple Grove, MN, USA: STABLEPOINT) have recently become available, and they will contribute to additional improvement in the quality of RFCA.

Several studies have suggested that LI decreases reflect tissue denaturation by RF applications, and the degree of LI drop is correlated with the lesion size. [12][13] [14] [15] However, although the LI can be changed by changing the catheter contact angle to the tissue, data on the effects of the catheter contact angle on LI parameters and lesion size are scarce. Therefore, this study aimed to evaluate the relationships among the catheter contact angles, LI parameters, and lesion size with 2 different LI-sensing ablation catheters in a porcine experimental study.

Methods

Ablation catheter and local impedance measurements

An open-irrigated MiFi ablation catheter with a 4.5 mm distal tip and an open-irrigated STABLEPOINT ablation catheter with a 4.0 mm distal tip were used for the experiment. The MiFi has 3 microelectrodes incorporated within the distal tip electrode, and there are 3 equally spaced 0.8 mm diameter microelectrodes located 2 mm from the tip of the catheter. First, LI was measured between each microelectrode and the 4^{th} ring electrode of the ablation catheter by a driven nonstimulatory alternating current (5.0 ?A, 14.5 kHz) between the distal tip electrode and the 4^{th} ring electrode to create a local potential field. After that, only the maximum LI was selected for the actual LI. Since the CF cannot be measured in the MiFi catheter, it was measured using the pressure-current transducer (load cell), as described in the next section. On the other hand, the STABLEPOINT does not have microelectrodes, and the LI was measured between the whole distal tip (4 mm length) and 2^{nd}ring electrodes by being driven by a nonstimulatory alternating current (5.0 ?A, 14.5 kHz) between the distal tip electrode and the 4^{th} ring electrode to create a local potential field.

In vitro experimental setup

Fresh porcine hearts were commercially obtained, which were extracted within 48 hours of sacrifice. Porcine myocardial tissue was fixed on a stage in a water pool (Figure 1). The saline solution was prepared for the water pool with 20 g of salt to 7.8 L of water so that the baseline LI was set at 90 ohms when using MiFi and 140 ohms when using STABLEPOINT because blood pool data for those catheters in the clinical setting were approximately 80–100 ohms for the MiFi and 130–150 ohms for the STABLEPOINT. The saline solution in the water pool was kept at 37 °C using a thermostatic system (Thermo-Mate BF-400, Yamato Scientific Co., Ltd., Tokyo, Japan). The water bath was circulated across the myocardial tissue surface at a flow rate of 5 L/min to simulate blood flow. The shaft of the catheter was fixed to the pillar 10 mm from the 4^{th} ring electrode in the distal direction, and the CF on the catheter tip was measured over time by connecting the pillar to a load cell (DPU-2N, Imada Co., Ltd., Toyohashi, Japan). The voltage waveform from the load cell was recorded by a 16-bit digital coder (DP850, Yokogawa Electric Corp., Tokyo, Japan). A scale was used to calibrate the CF at the tip of the catheter with the load cell voltage value in a range of 0–30 g.

Ablation protocol

RF lesions were created on the LV epicardium with a Rhythmia HDx Mapping System (Boston Scientific, Maple Grove, MN, USA). The RF application was delivered with a constant power of 30 watts and a duration of 30 seconds. CF (0, 5, 10, 20, and 30 g) and the catheter contact angle (30deg, 45deg, and 90deg) were changed in each set (total 120 lesions, n=8 each, Figure 2). The same experiment was performed with 2 different ablation catheters. The LI increases as the catheter contacts the tissue, and the LI decreases with the RF application. We defined the value of the LI increase above the baseline LI by the catheter contact as the LI rose and the absolute decrease in LI by the RF application as the LI dropped. The proportional values of the LI parameters were also evaluated to compare the 2 different catheters. The %LI rise was calculated as the LI rise divided by the baseline LI, and the %LI drop was calculated as the LI drop divided by the baseline LI.

RF lesion creation and measurement

After the RF application, the lesions were cut out and cross-sectioned at the center of the surface lesion, and macro images were taken. The maximum lesion width, surface width, and lesion depth were measured in each lesion (Figure 3) by the image analysis software ImageJ (NIH Image, Bethesda, MD). The average values measured by two persons were adopted to ensure objectivity.

Statistical analysis

All statistical analyses were performed using JMP 14 software (SAS Institute Inc., Cary, NC, USA). The data are presented as the mean +- standard error (SE) for continuous variables. The differences in lesion size (maximum lesion width, surface width, and lesion depth), LI rise, and LI drop among the three catheter angles were assessed by the analysis of variance in each CF, followed by post hoc analysis using the Tukey HSD test. The level of statistical significance was set at $p < 0.05$.

Results

LI rise and LI drop at different catheter contact angles

Figures 4A and 4C show the correlation between the catheter contact angle and the LI rise under each CF. The LI values increased as CF increased for both catheters. Regarding the difference in the catheter contact angles, there was no angular dependence for the LI rise under all CFs in the MiFi (Figure 4A). On the other hand, the LI rise at 90deg was lower than that at 30deg under 5 and 10 g of CF in STABLEPOINT (Figure 4C).

Figures 4B and 4D show the correlation between the catheter contact angle and the LI drop by the RF application under each CF. The LI drop values also increased as the CF increased for both catheters. Regarding the difference in the catheter contact angles, the LI drop at 90deg was significantly lower than that at 30deg under 10, 20, and 30 g of CF in the MiFi (Figure 4B). Likewise, the LI drop at 90deg was significantly lower than that at 30deg under 5, 10, 20, and 30 g of CF in STABLEPOINT (Figure 4D).

Relationship between catheter contact angle and lesion size

Figure 3 shows representative lesion images for each catheter angle RF application (30 watts, 30 seconds, 30 g of CF). Although the lesion depths were compatible, the maximum lesion widths and surface widths were smaller at 90deg than at 30deg and 45deg. The summarized data of all experiments are shown in Figure 5. In the MiFi group, the maximum lesion widths under 20 and 30 g of CF were smaller at 90deg than at 30deg and 45deg (CF 20 g: $P = 0.003$, CF 30 g: $P = 0.011$, respectively). Surface widths under 5, 10, 20, and 30 g of CF were also smaller at 90deg than at 30deg (CF 5 g: $P = 0.013$, CF 10 g: $P = 0.003$, CF 20 g: $P < 0.001$, CF 30 g: $P = 0.007$, respectively). On the other hand, the lesion depths were not significantly different among the three angles under any CF. For the STABLEPOINT, the maximum lesion widths under 0, 5, 10, 20 and 30 g of CF were smaller at 90deg than those at 30deg (CF 0 g: $P = 0.001$, 5 g: $P < 0.001$, 10 g: $P < 0.001$, 20 g: $P = 0.011$, and 30 g: $P = 0.039$, respectively). Surface widths under 0, 5, 10, 20, and 30 g of CF were also smaller at 90deg than at 30deg (CF 0 g: $P < 0.001$, 5 g: $P < 0.001$, 10 g: $P < 0.001$, 20 g: $P < 0.001$, and 30 g: $P = 0.032$, respectively). The lesion depths were not significantly different among the three angles under any CF.

Correlation between the LI drop and lesion size at each catheter contact angle

Figure 6 shows the correlations between the LI drop and lesion size at each catheter contact angle. The approximate curves were well fitted with a natural logarithm equation at all angles on the LI drop vs. the maximum lesion width (Figures 6A and 6C) and the lesion depth (Figure 6B and 6D) in the MiFi (upper) and STABLEPOINT (lower) models. Thus, the LI drops were correlated with maximum lesion widths and lesion depths at any angle for both ablation catheters.

Differences in the impact of the LI drop and lesion size between MiFi and STABLEPOINT

Comparing the 2 different catheters, the % LI rise in the STABLEPOINT was significantly higher than that in the MiFi under all CFs and all contact angles (Supplemental Figures A, B, and C). The values of % LI drop in the STABLEPOINT were significantly higher than those in the MiFi except for under 30 g of CF at 90deg and 45deg (Supplemental Figures D, E, and F).

Figure 7 shows the correlations between the %LI drop and lesion size for the 2 catheters. The approximate curves were well fitted with a natural logarithm equation on %LI drop vs. maximum lesion width (Figure 7A) and lesion depth (Figure 7B) for both catheters. The absolute values of the LI parameters were different, but the association between the percent changes and lesion sizes were similar between the 2 catheters.

Discussion

In this in vitro study, we evaluated the impact of the catheter contact angles on lesion formation, focusing on the LI parameters with different CFs in the 2 different LI-sensing ablation catheters. The major findings of our study are as follows: 1) the LI rose as CF increased, and the degrees of LI rise were not significantly different among the 3 catheter contact angles in the MiFi but it was lower at 90deg with the STABLEPOINT than at 30deg; 2) the LI drop at 90deg was lower than at 30deg for both ablation catheters; 3) the maximum lesion widths and surface widths were smaller at 90deg than at 30deg, whereas there were no differences in the lesion depths for both ablation catheters, 4) the actual value of the LI drops by the RF application were well correlated with the lesion sizes for each catheter angle, and 5) the %LI drops were predictable for lesion formation irrespective of the catheter angles for both ablation catheters.

Correlation between the lesion size and the catheter contact angles

Several studies have demonstrated that the catheter contact angle is an important factor in lesion creation.[16][17][18] In an in vitro study, Calzolar et al. reported [17] that the superficial lesion widths were increased by shifting the catheter angle from the perpendicular to the parallel orientation, and the intratissue maximal lesion widths were greater with an oblique catheter orientation than with a perpendicular position using a 3.5-mm tip, open-irrigated, CF-sensing catheter (TactiCath SE; Abbott, St. Paul, MN, USA). Conversely, they also reported that the lesion depths were not different with different catheter orientations. In the present study, the maximum lesion widths and surface widths were also smaller at 90deg than at 30deg, whereas there were no differences in lesion depth. Although the distal tip lengths of the ablation catheters are different (4.5 mm in INTELLANAV MiFi OI, 4.0 mm in INTELLANAV STABLEPOINT, and 3.5 mm in TactiCath SE), resulting in different sizes of the lesion creation,[19][20] their impact on the catheter angles are consistent with a previous study.

LI-guided RFCA considering the lesion size and interlesion distance

In RFCA for AF, PVI is the most effective procedure,[1] and the creation of secure RF lesions avoiding conduction gaps is essential to achieve a durable PVI.[21] [22] Recently, the Rhythmia module with an LI-sensing catheter was developed as a unique concept to determine the lesion size by the RF application. LI drops have been reported to be superior for predicting lesion size than FTIs [12] [15], and LI-guided PVI can provide a sufficient RF application along with the characteristics of the local myocardial tissue. Das M et al. reported that the optimal threshold of the LI drop for predicting gaps for anterior/roof segments was 16.1 ohms (positive predictive value for block: 96.3%) and for posterior/inferior segments it was 12.3 ohms (positive predictive value for block: 98.1%) with MiFi.[23] Our present study suggested that the lesion formation and LI parameters were changed by the different catheter angles (Figures 4 and 5). The LI drop and maximum lesion width at 90deg were significantly lower and smaller than those at 30deg, although lesion depths were not different among the three angles. This result suggests that the LI drop accurately reflects the difference in the lesion widths as the lesion volume changes with a perpendicular contact angle. Although indices such as FTI, LSI, and AI have been reported as useful parameters to predict RF lesion formation, it is impossible to recognize the differences in actual lesion formation (depth and width) by the catheter angle, which were observed in the present study. Therefore, LI-guided RFCA would allow us to adjust the ablation strategy, such as an optimal interlesion distance, to create continuous linear lesions considering the lesion widths.

Differences in the impact of the contact angle between MiFi and STABLEPOINT

In the present study, we evaluated 2 different LI-sensing ablation catheters. Notable differences between the 2 catheters for the LI were that the LI rise at 90deg was lower than at 30deg under 5 and 10 g of CF for the STABLEPOINT (Figure 4C), while there were no angular dependences for the LI rise under all CFs in the MiFi (Figure 4A). These results could be explained by the differences in the features of the 2 electrodes measuring the LI in each catheter. In the MiFi, the LI was measured between 3 microelectrodes and the 2nd ring electrode, and only the maximum LI was selected as the actual LI. On the other hand, the STABLEPOINT does not have a microelectrode, so the LI was measured between the whole distal tip and the 2nd ring electrode. Therefore, the tissue contact area or distance from the tissue to the LI measuring electrodes would be changed by the catheter contact angles. Therefore, the LI in STABLEPOINT would be affected by a larger area than for MiFi. In other words, the LI change affected by the myocardial tissue would be relatively smaller, especially with the more perpendicular catheter angle for STABLEPOINT, resulting in angular differences in the LI rise. In contrast, LI in the MiFi would be affected by a smaller area, i.e., the LI parameters in the MiFi would be more sensitive to tissue information. As a result, it is considered better to have a microelectrode to acquire more local LI information.

Since the size of the distal tips of STABLEPOINT was smaller (4 mm) than that of the MiFi (4.5 mm), the lesion sizes were larger for STABLEPOINT. Therefore, the %LI drop and %LI rise values (Supplemental Figure) were due to the different features of the catheters. On the other hand, the approximate curves were well fitted with the natural logarithm equation of %LI drop vs. maximum lesion widths (Figure 7A) and lesion depths (Figure 7B) for the 2 catheters. The absolute values of the LI parameters were different, but the association between the percent changes of the LI drop and lesion size were similar between the 2 catheters; therefore, the %LI drop can be a useful value for the concept of an LI-guided RFCA.

Clinical implications

There are few studies on LI drops by RF applications and lesion size considering the catheter contact angle. We found that the LI drop was an important factor for creating an effective RF lesion with 2 different LI-sensing catheters. In addition, we demonstrated that the catheter contact angles affected the LI drop and lesion size. The results of this study would be helpful to create effective RF lesions with a comprehension of the LI drop at each catheter angle.

Study limitations

Our study has several limitations. First, the CF cannot be directly measured with the INTELLANAV MiFi OI. Although the CF was measured with a digital scale with a calibrated force-current transducer (load cell), the actual CF might be different. Second, we evaluated the relationship between the LI drop, LI rise, and lesion size at different catheter angles under constant power and time; therefore, different settings were not evaluated. In addition, there was no steam pop during this study, so the predictive LI value for safety concerns could not be evaluated. Finally, since this experiment was performed in porcine myocardial tissues, the results may not be directly translated into clinical practice. RF lesion size in a clinical setting might be affected by multiple factors, such as stability, respiratory motion, or blood flow, not only catheter orientation. Therefore, clinical studies are necessary to assess lesion creation in a more clinically relevant setting.

Conclusion

The values of LI drop and lesion width at 90deg were significantly smaller than those at 30deg at the same ablation setting, although the lesion depths were not different among the 3 angles for the MiFi and the STABLEPOINT. They were correlated with maximum lesion width and lesion depth at any angle, which could be a good predictor of the lesion size by RF applications.

Acknowledgments

We would like to thank Yoshiki Tasaki and Masaya Mizokami for their help with this work.

Disclosure

This study received no financial support from commercial sources, and the authors have no conflicts of interest to declare.

References

1. Parkash R, Tang AS, Sapp JL, Wells G. Approach to the Catheter Ablation Technique of paroxysmal and Persistent Atrial Fibrillation: A Meta-Analysis of the Randomized Controlled Trials. J Cardiovasc Electrophysiol 2011;22:729-738.
2. Viles-Gonzalez JF, Berjano E, d'Avila A. Complications of Radiofrequency Catheter Ablation: Can We Prevent Steam Pops?. JACC Clin Electrophysiol 2018;4(4): 501-503.
3. Reddy VY, Shah D, Kautzner J, Schmidt B, Saoudi N, Herrera C, Jais P, Hindricks G, Peichl P, Yulzari A, Lambert H, Neuzil P, Natale A, Kuck KH. The relationship between contact force and clinical outcome during radiofrequency catheter ablation of atrial fibrillation in the TOCCATA study. Heart Rhythm 2012;9(11):1789-1795.
4. Kimura M, Sasaki S, Owada S, Horiuchi D, Sasaki K, Itoh T, Ishida Y, Kinjo T, Tomita H, Okumura K. Comparison of lesion formation between contact force-guided and non-guided circumferential pulmonary vein isolation: A prospective, randomized study. Heart Rhythm 2014;11(6):984-991.
5. Neuzil P, Reddy VY, Kautzner J, Petru J, Wichterle D, Shah D, Lambert H, Yulzari A, Wissner E, Kuck KH. Electrical Reconnection After Pulmonary Vein Isolation Is Contingent on Contact Force During Initial Treatment: results from the EFFICAS I study. Circ Arrythm Electrophysiol 2013;6(2):327-333.
6. Shah DC, Lambert H, Nakagawa H, Langenkamp A, Aeby N, Leo G. Area under the real-time contact force curve (force-time integral) predicts radiofrequency lesion size in an in vitro contractile model. J Cardiovasc Electrophysiol 2010;21:1038-1043.
7. Phlips T, Taghji P, El Haddad M, Wolf M, Knecht S, Vandekerckhove Y, Tavernier R, Duytschaever M. Improving procedural and one-year outcome after contact force-guided pulmonary vein isolation: the role of interlesion distance, ablation index, and contact force variability in the 'CLOSE'-protocol. Europace 2018;20:419-427.
8. Hussein A, Das M, Chaturvedi V, Asfour IK, Daryanani N, Morgan M, Ronayne C, Shaw M, Snowdon R, Gupta D. Prospective use of ablation index targets improves clinical outcomes following ablation for atrial fibrillation. J Cardiovasc Electrophysiol 2017;28(9):1037-1047.
9. Calzolari V, De Mattia L, Indiani S, Crosato M, Furlanetto A, Licciardello C, Squasi P Antonio M, Olivari Z. In vitro validation of the lesion size index to predict lesion width and depth after irrigated radiofrequency ablation in a porcine model. JACC Clin Electrophysiol 2017;3(10):1126-1135.
10. Reichlin T, Kecht S, Lane C, Kuhne M, Nolf E, Chopra N, Tadros TM, Reddy VY, Schaer B, John RM, Osswald S, Stevenson WG, Sticherling C, Michaud GF. Initial impedance decrease as an indicator of good catheter contact: Insights from radiofrequency ablation with force sensing catheters. Heart Rhythm 2014;11(2):194-201.
11. Garrott K, Gams A, Laughner J, Lehn L, Gutbrod S, Hamann J. Local impedance on a force sensing catheter predicts volumetric lesion temperature changes. EP Europace. 2020;22.
12. Sulkin MS, Laughner JI, Hilbert S, Kapa S, Kosiuk J, Younan P, Romero I, Shuros A, Hamann JJ, Hindricks G, Bollmann A. Novel measure of local impedance predicts and catheter-tissue contact and lesion formation. Circ Arrythm Electrophysiol 2018;11(4): 005831.
13. Martin CA, Martin R, Gajendragadkar PR, Maury P, Takigawa M, Cheniti G, Frontera A, Kitamura T, Duchateau J, Vlachos K, Bourier F, Lam A, Load S, Murray S, Shephard E, Pambrun T, Denis A, Derval N, Hocini M, Haissaguerre M, Jais P, Sacher F. First clinical use of novel ablation catheter incorporating local impedance data. J Cardiovasc Electrophysiol 2018;29(9):1197-1206.
14. Gunawardene M, Münkler P, Eickholt C, Akbulak RÖ, Jularic M, Klatt N, Hartmann J, Dinshaw L, Jungen C, Moser JM, Merbold L, Willems S, Meyer C. A novel assessment of local impedance during catheter ablation: initial experience in humans comparing local and generator measurements. Europace

2019;21:34-42.

15. Garrott K, Laughner J, Gutbord S, Sugrue A, Shuros A, Sulkin M, Yasin O, Bush J, Pottinger N, Meyers J, Kapa S. Combined local impedance and contact force for radiofrequency ablation assessment. Heart Rhythm 2020;17(8):1371-1380.
16. Kawaji T, Hojo S, Kushiyama A, Nakatsuma K, Kaneda K, Kato M, Yokomatsu T, Miki S. Limitation of lesion quality estimated by ablation index: an in vitro study. J Cardiovasc Electrophysiol 2019;30(6):926-933.
17. Calzolari V, De Mattia L, Basso F, Crosato M, Scalon A, Squasi PAM, Del Favero S, Cernetti C. Ablation catheter orientation: In vitro effects on lesion size and in vivo analysis during PVI for atrial fibrillation. Pacing Clin Electrophysiol 2020;43(12):1554-1563.
18. Masnok K, Watanabe N. Relationship of Catheter Contact Angle and Contact Force with Contact Area on the Surface of Heart Muscle Tissue in Cardiac Catheter Ablation. Cardiovasc Eng Technol 2021;12(4):407-417.
19. Kawano D, Mori H, Kato R, Tsutsui K, Ikeda Y, Sumitomo N, Fukaya H, Iwagana S, Nakano S, Muramatsu T, Matsumoto K. The optimal ablation setting for a local impedance guided catheter in an in vitro experimental model. J Cardiovasc Electrophysiol 2021;32(8):2069-2076.
20. Yokoyama K, Nakagawa H, Shah DC, Lambert H, Leo G, Aeby N, Ikeda A, Pitha JV, Sharma T, Lazzara R, Jackman WM. Novel contact force sensor incorporated in irrigated radiofrequency ablation catheter predicts lesion size and incidence of steam pop and thrombus. Circ Arrythm Electrophysiol 2008;1(5):354-362.
21. Nery PB, Belliveau D, Nair GM, Bernick J, Redpath CJ, Szczotka A, Sadek MM, Green MS, Wells G, Birnie DH. Relationship between pulmonary vein reconnection and atrial fibrillation recurrence: a systematic review and meta-analysis. JACC Clin Electrophysiol 2016;2(4):474-483.
22. Verma A, Kilicaslan F, Pisano E, Marrouche NF, Fanelli R, Brachmann J, Geunther J, Potenza D, Martin DO, Cummings J, Burkhardt JD, Saliba W, Schweikert RA, Natale A. Response of atrial fibrillation to pulmonary vein antrum isolation is directly related to resumption and delay of pulmonary vein conduction. Circulation2005;112(5):627-635.
23. Das M, Luik A, Shepherd E, Sulkin M, Laughner J, Oesterlein T, Duffy E, Meyer C, Jais P, Duchateau J, Yue A, Ullah W, Ramos P, García-Bolao I. Local catheter impedance drop during pulmonary vein isolation predicts acute conduction block in patients with paroxysmal atrial fibrillation: initial results of the LOCALIZE clinical trial. Europace 2021;23(7):1042-1051.

Figure legends

Figure 1. In vitro experimental setup.

(A) The saline solution in the water pool was kept at 37 °C using a thermostatic system and it was driven across the surface of the myocardial tissue at a flow rate of 5 L/min to simulate blood flow. The solution in the water pool was adjusted to 90 and 140 ohms of baseline LI for MiFi and STABLEPOINT, respectively. (B) Lesions were created on the porcine myocardial left ventricles by 2 LI-sensing ablation catheters. (C) RFCA was performed with a constant power of 30 watts and a duration of 30 seconds. The CF and catheter contact angles were changed in each set.

LI = local impedance, CF = contact force, RFCA = radiofrequency ablation.

Figure 2 Ablation protocol

The study protocol is shown in Figure 2. A detailed explanation is given in the main text.

CF = contact force, RF = Radiofrequency.

Figure 3. RF lesion size measurement.

Figure 3 shows the representative lesion images for each catheter angle RF application (30 watts, 30 sec, CF = 30 g). MWs, SWs, and LDs were evaluated for each lesion.

MW = maximum lesion width, SW = surface width, LD = lesion depth, RFCA = radiofrequency ablation.

Figure 4. Relationship between the catheter contact angle and the LI rise and LI drop

Figure 4 shows the correlation between the catheter contact angle and LI rise (4A and 4C) and the LI drop (4B and 4D) under each CF in the MiFi (upper panel) and the STABLEPOINT (lower panel).

LI = local impedance, CF = contact force.

Figure 5. Relationship between the catheter contact angle and lesion size

Figure 5 shows the correlation between the catheter contact angle and lesion size.

In the MiFi, (A) MWs at 90° were smaller than those at 30° under 20 g and 30 g of CF; (B) SWs at 90° were smaller than those at 30° under 5, 10, 20, and 30 g of CF; (C) the LDs were not significantly different for each of the three catheter angles. In the STABLEPOINT, (D) MWs at 90° were smaller than those at 30° under 0, 5, 10, 20, and 30 g of CF; (E) SWs at 90° were smaller than those at 30° under 0, 5, 10, 20, and 30 g of CF; (F) LDs were not significantly different for each of the three catheter angles.

MW = maximum lesion width, SW = surface width, LD = lesion depth.

Figure 6. Correlation between the LI drop and lesion size at each catheter contact angle

The approximate curves were well fitted with a natural logarithm equation on LI drop vs. lesion size at all catheter angles. Thus, the LI drops by RF application were well correlated with the lesion sizes at each catheter angle.

MW = maximum lesion width, SW = surface width, LD = lesion depth.

Figure 7.

Differences in the impact of the contact angle between MiFi and STABLEPOINT

The approximate curves were well fitted with a natural logarithm equation on %LI drop vs. maximum lesion width (Figure 7A) and lesion depth (Figure 7B) for both catheters. The absolute values of the LI parameters were different, but the association between the percent changes and lesion size was similar for both catheters.

CF = contact force, %LI drop =LI drop/baseline LI.

Supplemental Figure

The difference in the %LI drop between the MiFi and STABLEPOINT

Comparing the 2 different catheters, the values of %LI rise for the STABLEPOINT were significantly higher than those for the MiFi under all CF and contact angles. The %LI drops for STABLEPOINT were significantly higher than those for MiFi except for under 30 g of CF at 90° and 45°.

CF = contact force, %LI rise =LI rise/baseline LI, %LI drop =LI drop/baseline LI.

Fig 1.

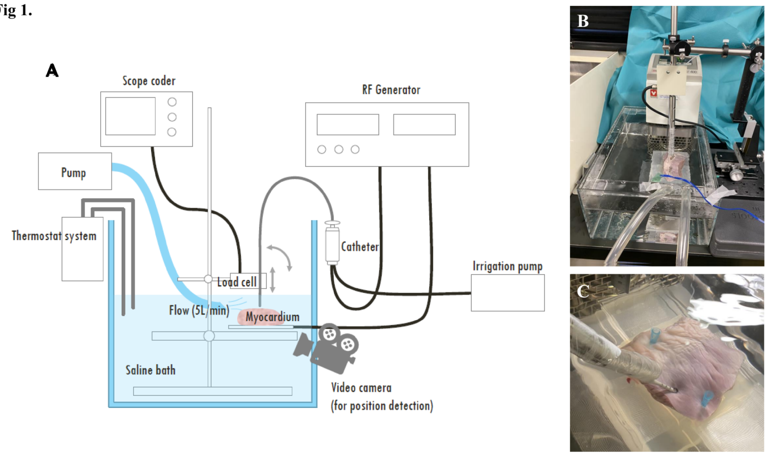

Fig 2.

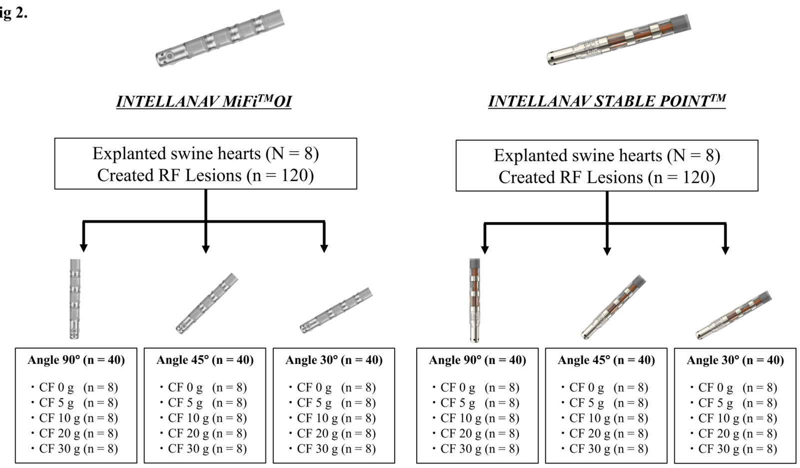

Fig 3.

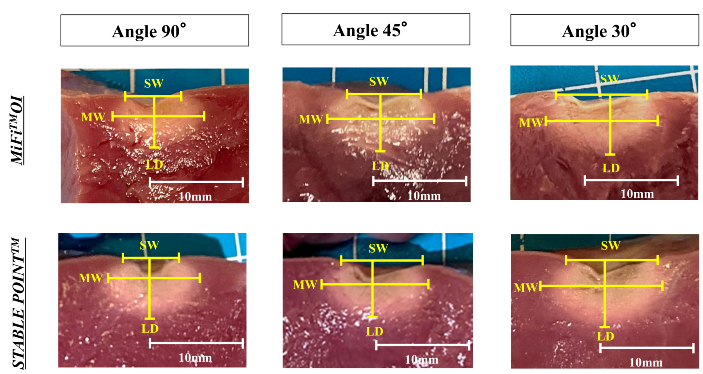

lesion size: MW = maximum lesion width, SW = surface width, LD = lesion depth.

Fig 4.

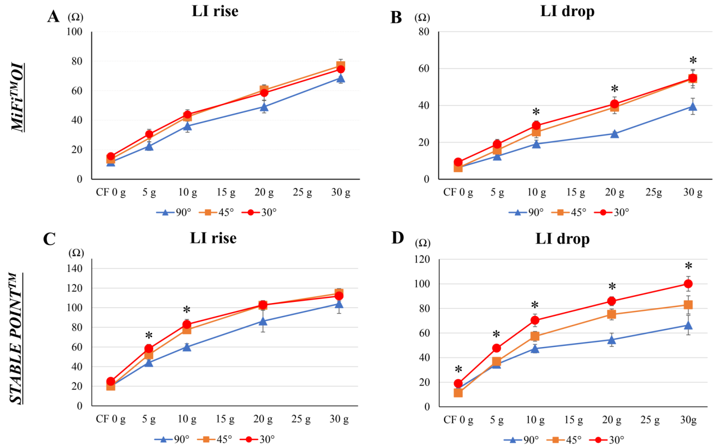

Data presented as the mean ± SE. Abbreviation: LI = local impedance, CF = contact force. * P < 0.05.

Fig 5.

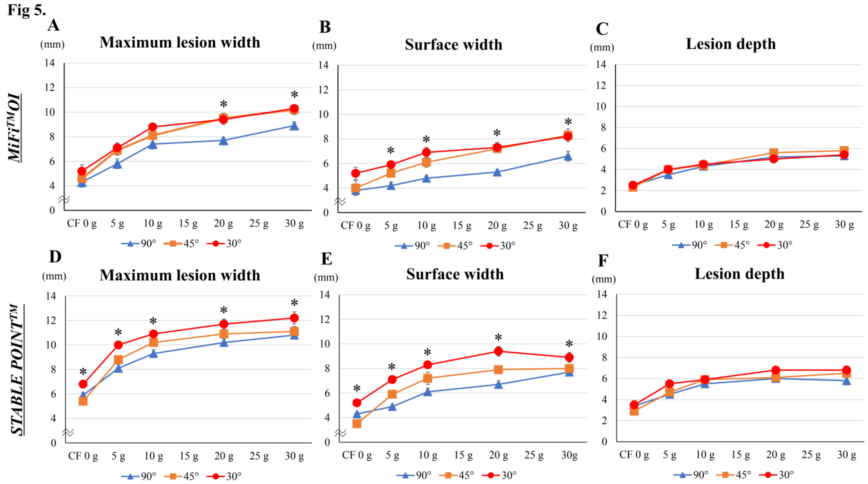

Fig6.

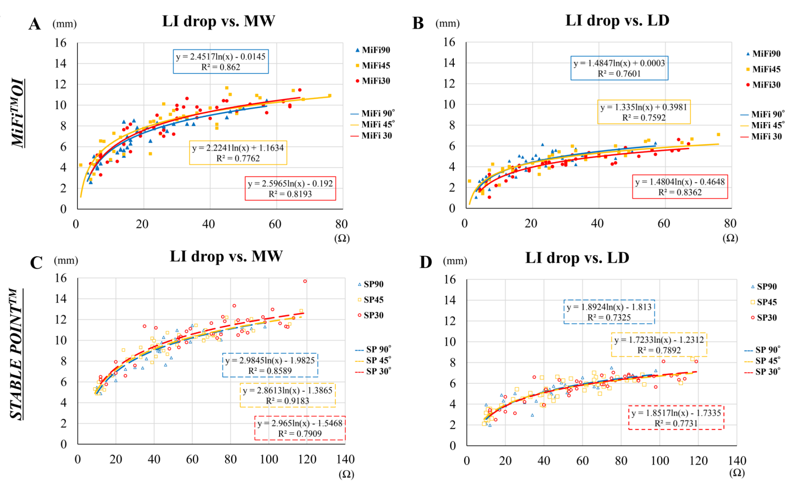

Fig 7.

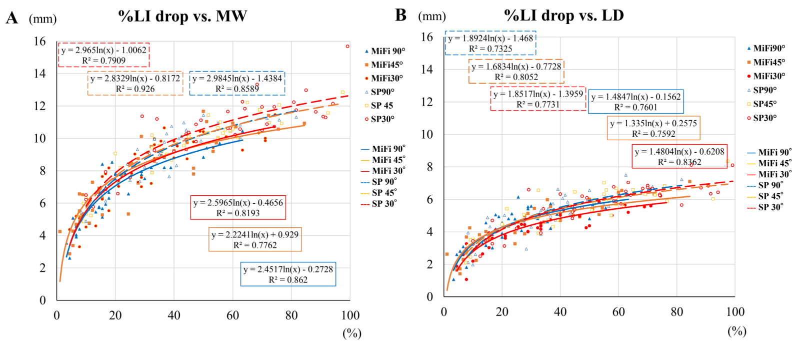

A
(mm)
%LI drop vs. MW
y = 2.965ln(x) - 1.0062
R² = 0.7909
y = 2.8329ln(x) - 0.8172
R² = 0.926
y = 2.9845ln(x) - 1.4384
R² = 0.8589
y = 2.5965ln(x) - 0.4656
R² = 0.8193
y = 2.2241ln(x) + 0.929
R² = 0.7762
y = 2.4517ln(x) - 0.2728
R² = 0.862
MiFi 90°
MiFi45°
MiFi30°
SP90°
SP 45
SP30°
MiFi 90°
MiFi 45°
MiFi 30°
SP 90°
SP 45°
SP 30°
(%)
B
(mm)
%LI drop vs. LD
y = 1.8924ln(x) - 1.468
R² = 0.7325
y = 1.6834ln(x) - 0.7728
R² = 0.8052
y = 1.8517ln(x) - 1.3959
R² = 0.7731
y = 1.4847ln(x) - 0.1562
R² = 0.7601
y = 1.335ln(x) + 0.2575
R² = 0.7592
y = 1.4804ln(x) - 0.6208
R² = 0.8362
MiFi90°
MiFi45°
MiFi30°
SP90°
SP45°
SP30°
MiFi 90°
MiFi 45°
MiFi 30°
SP 90°
SP 45°
SP 30°
(%)